Active Inverted Stripline Circular Patch Antennas for Spatial Power Combining

Julio A. Navarro, *Student Member, IEEE* Lu Fan, and Kai Chang, *Fellow, IEEE*

Abstract—**A new active antenna configuration is proposed for spatial power combining applications. The active patch antenna uses an inverted stripline topology to take advantage of several features. These features include avoiding drilling through the circuit substrate to insert the diode and the use of air within the resonant cavity for reducing loss. The inverted substrate can serves as a radome for hermetic sealing. The active antenna and housing can be fabricated in modular form for reduced cost and easy replaceability of devices. The active inverted stripline patch antenna exhibits a much cleaner spectrum and greater stability than previously reported active antennas. The fixture serves as a ground plane, heat sink, and support in an active planar array or as a mirror in a quasi-optical power combining resonator. A single active antenna operating at 9.23 GHz exhibited a 16 MHz locking bandwidth at 30 dB locking gain. Power combining efficiencies of over 89% have been demonstrated for a four element square array. The square array maintained injection-locking and power combining over a 60 MHz bias tuned bandwidth. Similarly, a four element diamond array showed over 86% combining efficiency and 50 MHz bias tuned bandwidth. Beam Steering was demonstrated by varying bias voltage to the individual antenna elements of the square array.**

I. Introduction

ACTIVE ANTENNAS with spatial power combining techniques have been devised to overcome low power levels and fabrication costs of mm and sub-mm wave systems. By designing the antenna and oscillator on a single substrate, one avoids transition/transmission line losses from power distribution networks and moves closer towards complete monolithic integration. At mm and sub-mm wavelengths, monolithic construction becomes necessary to overcome many fabrication difficulties. However, solid-state devices produce very small power levels at these frequencies while waveguide dimensions and tolerances become difficult and costly for circuit-level power combining. The use of active antennas and spatial or quasi-optical power combing techniques can overcome these limitations [1], [2]. General power combining techniques are reviewed in [1] while the current state of quasi-optical power combining technology is described in [3].

Active antennas are those radiators directly integrated with active devices to generate RF power. Active antennas have been realized using two terminal and three terminal devices. FETs and other three terminal solid-state devices have shown higher DC to RF conversion efficiencies over two terminal devices. However, diodes reach much higher operating frequencies. The active antenna provides a tank circuit, matching transformer or feed back mechanism to sustain oscillations. A group of active antennas can be injection-locked for phase-coherency and power combining.

The microstrip patch antenna has been integrated with diodes and transistors for active, planar, low-cost radiating elements [4]–[8]. The microstrip structure provides a resonant patch for oscillations and a ground plane for efficient heat sinking. However, the patch has exhibited narrow bias tuning ranges, high cross-polarization levels, and wide output power deviations. A tuning diode and bipolar transistor has recently been integrated within a *multi-layer* patch to obtain 4.4% tuning of the operating frequency [9]. As an alternative, the endfire notch has many desirable characteristics including broad impedance matching bandwidth, uniplanar nature and easy integration of other planar solid-state devices. Its scalability is attractive for use well into the sub-mm wave region. Active varactor tunable notch antennas have been reported [10]–[12]. However, an array of such endfire antennas would require a brick style approach for power combining arrays. Although the brick style approach offers large heat dissipation volume and circuit area with modular replaceability of components, it tends to be bulkier than an array using a tile style method. For tile type approaches in power combining, endfire elements may not be as suitable as broadside microstrip patches, bowties, grids and dipoles.

Power combining methods enable arrays of active antennas to operate as one coherent transmitter with predictable effective radiated power, beamwidth and tuning bandwidth. Power-combining techniques include chip-level, circuit-level and spatial combiners. Spatial and open resonator combiners involve a large number of transistors or diodes. The individual free-running oscillators must be injection-locked to produce a coherent higher power RF source. Injection locking may be obtained via mutual coupling, external feedback, or an external source. The result of using spatial or quasi-optical power combining techniques is to create a single, coherent and higher-power signal from many low-power radiating sources. Spatial or quasi-optical power combining is not as limited by size, ohmic or dielectric losses or moding problems and allows the combination of a greater number of active devices. The patch and grid have been used for most active antennas and in power combining [13]–[17].

This paper introduces the cavity-enclosed inverted stripline circular patch antenna. This antenna structure does not require drilling through the circuit substrate to accommodate diodes. Drilling on the housing is still required but is not as critical. A

Manuscript received August 18, 1992; revised March 19, 1993.

The authors are with Texas A&M University, Electrical Engineering Department, College Station, Texas 77843-3128.

IEEE Log Number 9211937.

housing has been designed so that the feed or diode position is easily optimized. The configuration's enclosure chokes out surface waves and introduces an increase in metal volume for heat dissipation. DC bias is provided to the diode from the ground plane side with a feed-through capacitor. This scheme does not require direct contact with the patch radiator and can improve the impedance match to the diode. The inverted stripline active patch antenna can also be integrated with other solid-state devices for increased power, frequency switching and/or tuning. The axial symmetry of the antenna can be used for circuit level power combining with more than one active device placed under the patch radiator [18]. Monolithic integration of such an antenna in a tile type planar array could be accomplished with monolithic chip inserts at each antenna location. Each insert would contain the patch and active devices.

The active inverted stripline patch exhibits a purer spectrum than previously reported active antennas with improved stability and external Q-factor. The antenna can be optimized for improved diode matching and increased diode power output as in waveguide cavities. Injection-locking experiments on a single active antenna show a locking bandwidth 16 MHz at a locking gain of 30 dB. E and H-plane power combining arrays show high combining efficiencies. A four element square array with 89% combining efficiency showed an injection-locked bias tuning bandwidth of 60 MHz. Similarly, a four element diamond array showed over 86% combining efficiency and 50 MHz bias tuned bandwidth.

II. Circuit Design and Description

The cavity-enclosed inverted stripline antenna dimension parameters are shown in Fig. 1(a). The inverted patch is enclosed by a cylindrical air-filled cavity. The antenna radiates through a short section of dielectric-filled circular waveguide to free space. References [19] and [20] describe design formulations which were applied to this inverted stripline structure design. This structure and a coaxial probe were used to create a passive antenna.

Since the probe-fed antenna is inverted and enclosed, soldering the coaxial probe to the patch is difficult and avoided. Instead a cap on the probe is used to capacitively couple to the antenna. The cap used is equal to the Gunn diode cap diameter in anticipation of the active antenna application. Some of the passive antenna design aspects worth noting include that: the inverted substrate serves as a radome, no drilling through the circuit or soldering to the patch is required, thick antenna dimensions are allowed without surface wave losses.

A test fixture was designed to allow experimental optimization of the passive and active design. The enclosure allows the use of dielectric inserts to test different patch antenna diameters on different substrate thicknesses or dielectric constants. Fig. 1(b) shows the passive probe-fed cavity-enclosed inverted stripline configuration. Several probe-fed antennas were tested using the following parameters:

- Cavity Diameter (C) = 12.700 mm.
- Substrate Thickness (a) = 1.524 mm and $\varepsilon_2 = 2.3$.
- Air Spacing (b) = 1.500 mm and $\varepsilon_1 = 1.0$.

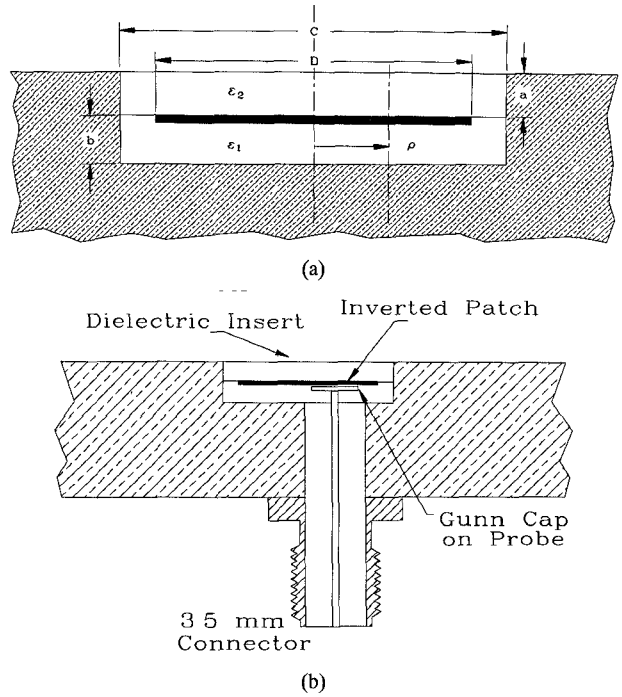

Fig. 1. The cavity-enclosed inverted stripline antenna: (a) Structure dimensions. (b) The passive probe-fed antenna configuration.

TABLE I
MEASURED AND CALCULATED OPERATING FREQUENCIES OF SEVERAL PATCH ANTENNAS

Patch Diameter (mm)	Calculated f_r (GHz)	Measured f_r (GHz)	% Error
8	13.300	13.30	0
9	12.285	12.35	−0.50
10	11.415	11.00	3.77
10.4	11.101	10.70	3.75
11	10.661	10.10	5.56

- Patch Diameters (D) = 8, 9, 10, 10.4 and 11 mm.
- 3.5 mm connector (Gunn diode cap on probe).
- Probe Position (ρ) = 2 mm.

Patch antennas with different diameters were etched on RT-Duroid 5870 with a 1.524 mm thickness and ε_r of 2.3. The antennas were concentrically cut-out in 12.7 mm diameter inserts for the cavity enclosure. Several dielectric inserts were tested for return loss on an HP-8510B Network Analyzer. Instead of soldering a probe feed to the antenna, a circular disk over the probe tip was used to simulate the Gunn diode cap of the active antenna application as shown in Fig. 2. This cap is also used as a proximity feed to tune out some of the probe's inductive effect. Table I lists computed and measured operating frequencies for several patch antennas of different diameters.

Table I shows a deviation of antenna resonance for larger patch diameters. As the patch diameter increases, the distance between the radiating edges and the enclosure decrease well within a ground plane spacing causing a lower resonance frequency. Our current formulation based on [19] and [20] does

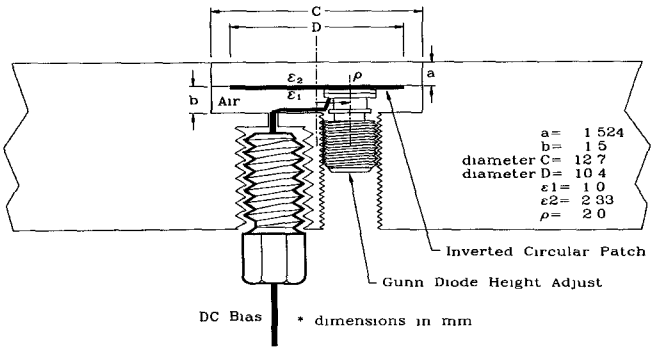

Fig. 2. The cavity-enclosed active inverted stripline antenna with Gunn diode and bias scheme.

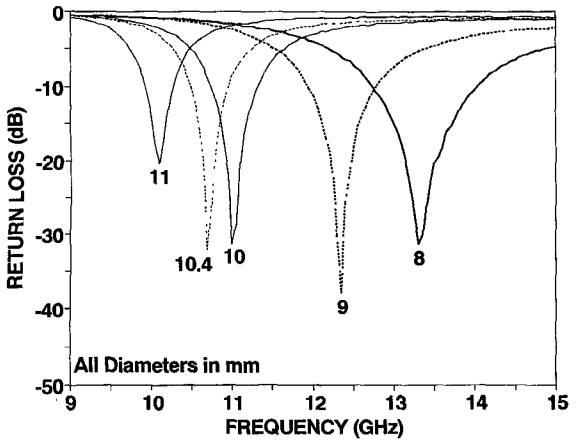

Fig. 3. The measured return loss for various patch diameters of the probe-fed passive antenna.

not account for the cavity enclosure effect on the resonance of the inverted patch antenna. Fig. 3 shows the measured return loss of several cavity-enclosed probe-fed inverted stripline antennas.

The probe-fed passive antenna radiation patterns were used to determine beamwidth, cross-polarization and gain level. The gain of the cavity-enclosed inverted stripline circular patch antenna is 6.65 dBi. This gain level is used later to approximate Gunn oscillator power in the active antenna. The E-plane 3 dB beamwidth is over 105 degrees. The H-plane 3 dB beamwidth is 80 degrees. Cross polarization levels remain at least 16 dB below the maximum on either H or E-plane patterns. Fig. 4 shows the radiation patterns for a 10.4 mm diameter probe-fed cavity-enclosed inverted stripline antenna. E-plane pattern modulation or ripple is caused by the edges of a relatively small fixture.

III. A Single Active Antenna Element

The active antenna design addresses heat dissipation and hermetic sealing concerns of active applications. Heat dissipation is specially important at higher frequencies where devices are less efficient and circuit dimensions are reduced. Fixtures or housings serve as structural support, electrical ground planes and heat sinks which dissipate heat away from active devices. This antenna includes a cavity enclosure [21] which chokes out surface waves and further increases the metal volume for heat

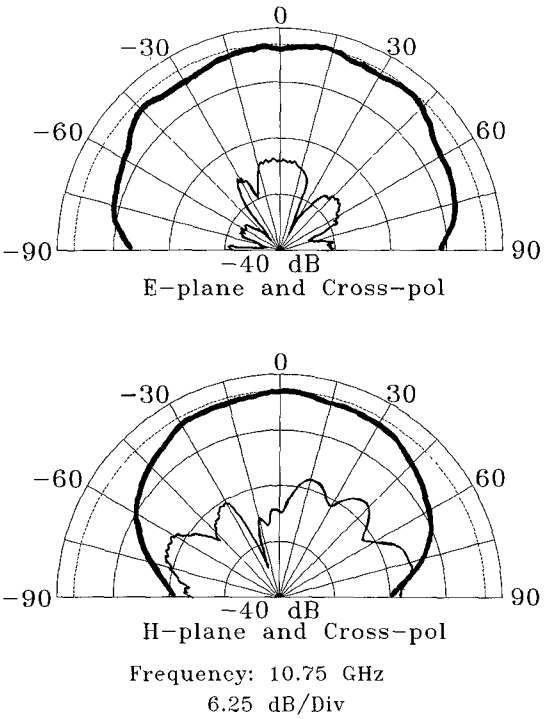

Fig. 4. The probe-fed passive antenna radiation patterns.

TABLE II
Measured Active Antenna Operating Frequency and Oscillator Power

Inverted Patch Diameter (mm)	Operating Frequency: F_0 (GHz)	Gunn Oscillator Power* (GHz)	EIRP (mW)
8	9.997	63.99	295.88
9	9.637	56.76	262.45
10	9.438	57.04	263.74
10.4	9.240	63.98	295.83
11	8.908	66.98	309.70

*Calculated using a passive antenna gain of 6.65 dBi.

dissipation. For hermetic sealing, the inverted stripline antenna insert can have matched thermal expansion coefficients with the alloy used to make the housing. The matched thermal expansion coefficients will reduce stresses and cracks in hostile environments to maintain hermeticity, increase durability and improve reliability of active devices [22].

The active cavity-enclosed inverted stripline antenna uses a screw-type diode fastened to a large base plate as shown in Fig. 2. The cavity enclosure is placed around the diode and fastened to the base plate. A circular patch antenna etched on a circular RT-Duroid dielectric insert is pressed into the cavity enclosure over the diode. The inverted patch serves as a resonant circuit for the Gunn diode. Biasing to the diode can be etched on the dielectric insert or applied through a filtering capacitor below the ground plane.

The input impedance of the antenna can be used with the equivalent circuit for the Gunn diode to determine the active antenna oscillation frequency. The Gunn diode, when biased above its threshold voltage, will oscillate if it sees a real impedance less than or equal to its own in a circuit. The

TABLE III
OPERATING FREQUENCIES AND OSCILLATOR POWER VS. GUNN BIAS VOLTAGE

Bias Voltage (Volts)	Operating Frequency F_0 (GHz)	Gunn Oscillator Power* (mW)	EIRP (mW)
8	9.003	28.31	130.90
9	9.036	38.02	175.80
10	9.067	52.64	243.40
11	9.096	60.20	278.35
12	9.119	62.93	290.98
13	9.134	67.99	314.37
14	9.143	70.56	326.26
15	9.143	75.42	348.73

*Calculated using a passive antenna gain of 6.65 dBi.

condition is depicted by the following equation:

$$|\mathrm{Re}[Z_g]| \geq \mathrm{Re}[Z_c] \tag{1}$$

where $\mathrm{Re}[Z_g]$ is equal to the real part of the Gunn diode negative resistance $(-R_g)$ and Z_c is the circuit impedance. The operating frequency occurs when the overall imaginary impedance components cancel out

$$\mathrm{Im}[Z_g] + \mathrm{Im}[Z_c] = 0 \tag{2}$$

A screw type Gunn diode form M/ACOM 49106-111 was used with typical output power levels of over 50 mW. Increasing patch antenna diameter causes an inversely proportional shift in the active antenna oscillation frequency. The Gunn oscillator power output of the active antenna was calculated from the received power using the Friis transmission formula as described in [11], [12], [14]. The measured gain of the passive probe-fed antenna was used to approximate active antenna element's gain. Table II lists active antenna operating frequencies and oscillator power with respect to patch size. The effective isotropic radiated power (EIRP) is also included for comparison with other power combiners.

One could supply DC bias to the patch conductor and then make contact with the diode. Our design biases the diode directly from under the ground plane using a filtering capacitor. This biasing scheme allows proximity coupling to the patch antenna to tune out some of the diode's series inductive component. One can use the method to experimentally tune over a small range of frequencies for a given mode. An electronic method of varying the frequency of operation involves the bias voltage. Varying the bias voltage of the Gunn diode causes a change in the diode junction reactance and a corresponding shift in operating frequency. Table III lists typical Gunn bias voltages vs. operating frequencies and oscillator power for the active antenna. The overall tuning range of the active antenna is 140 MHz. The 3 dB bias tuning range is 107 MHz at 9.09 GHz or 1.2%. The active antenna pattern remains well-behaved with a cross-polarization level of at least 10 dB below the maximum.

The active antenna spectrum is very pure, stable and comparable to waveguide oscillators. The high external quality factor is due to the small cylindrical enclosure surround the inverted stripline antenna. The cylindrical enclosure stabilizes the oscillating frequency and reduces surface mode losses. The

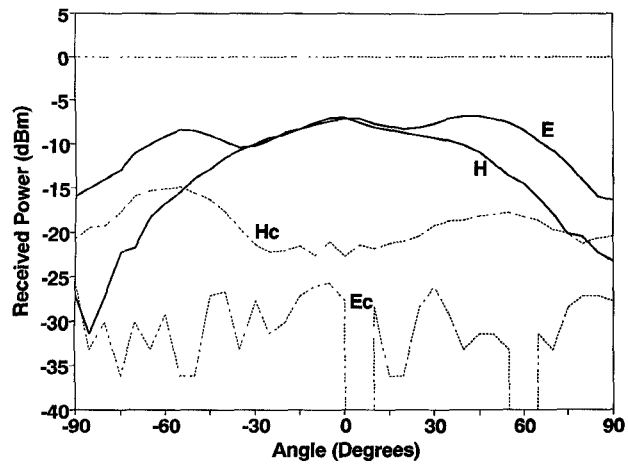

Fig. 5. the active antenna radiation patterns with the Gunn diode located 2 mm off-center. (E, H-co-polarization; E_c, H_c-cross-polarization.)

Gunn diode's vertical proximity to the patch was used to tune over a small frequency range. This mechanical adjustment was useful in ensuring that several antennas would operate at the same bias voltage and within the small locking bandwidth when power combining via mutual coupling.

The Gunn diode's position under the antenna changes the real and imaginary impedance presented to its terminals thereby altering the operating frequency. The Gunn diode oscillates at different radial distances including at the patch center. However, since the active antenna pattern is strongly dependent on diode position, centering diode causes a broadside null to appear with a well-behaved conical beam similar to a vertical monopole. When the diode is off center, the pattern is broadside. The cross polarization level is at least 10 dB below the maximum for a Gunn diode 2 mm off-center. Typical radiation patterns for the active antenna are shown in Fig. 5. The 3 dB beamwidth is 100 and 70 degrees for the E and H-plane, respectively. The cross-pol level is 10 dB below the maximum. This compares favorably with the passive antenna patterns of Fig. 4. Differences in beamwidth and cross-pol levels may be attributed to differences in antenna perturbation between the probe and Gunn diode package.

IV. INJECTION LOCKING

External injection-locking experiments with an HP-83622A synthesized sweeper were performed to determine the locking-

TABLE IV
OPERATING FREQUENCY, OSCILLATOR POWER AND EFFICIENCY OF EACH ANTENNA AND ARRAY

Antenna	1	2	3	4	Square Array*	5	6	7	8	Diamond Array**
Oscillator Frequency (GHz)	9.498	9.499	9.498	9.497	9.511	9.330	9.340	9.330	9.340	9.380
Oscillator Power (mW)	52.63	56.80	59.32	60.14	204	50.55	49.51	56.72	55.55	184
EIRP (mW)	243.4	262.6	274.3	278.1	3773	233.7	228.9	262.3	256.8	3403
[dBm]	[23.9]	[24.2]	[24.4]	[24.4]	[35.8]	[23.7]	[23.6]	[24.2]	[24.1]	[35.3]
Combining Efficiency (%)	—	—	—	—	89.03	—	—	—	—	86.57
DC to RF Efficiency (%)	1.75	1.89	1.98	2.00	1.63	1.69	1.65	1.89	1.85	1.47

*Antennas 1, 2, 3, and 4 are used in the Square Array with 17 mm Spacing.
**Antennas 5,6,7, and 8 are used in the Diamond Array with 17 mm Spacing along the diagonal.

gain and locking-bandwidth of the active antenna. The test measurement set-up is described in [11], [14]. The signal quality shows a noticeable improvement in noise level and spectral purity after injection-lock.

The locking gain ($G_L = P_{\text{output}}/P_{\text{injected}}$) determines the relative power required to externally injection lock the active antenna element. A 10.4 mm patch exhibited a locking gain of 30 dB, a locking bandwidth of 16 MHz at 9.23 GHz. As the injection lock signal power decreases, there is a corresponding decrease in obtainable locking bandwidth. The external Q-factor of the circuit is found using equation given in [23]. The external Q-factor of the active cavity-enclosed inverted stripline antenna was computed at 36. In comparison with previous active antennas of [12] and [14], this external Q-factor is nearly doubled.

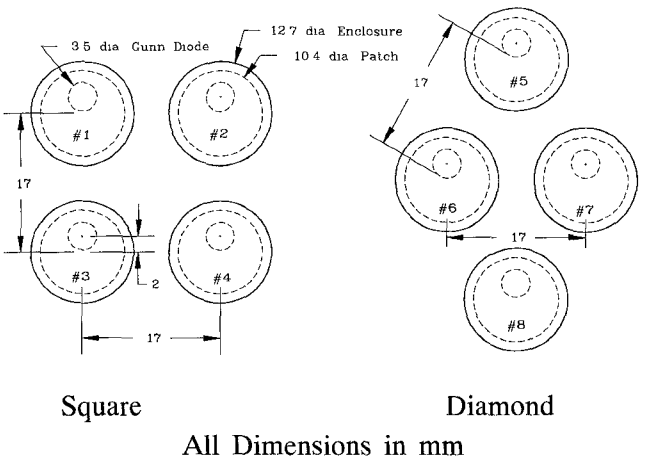

Fig. 6. Array configurations and spacing.

V. POWER COMBINING

The power combining concept uses many low power sources to provide a single coherent, higher power output. To demonstrate spatial power combining via mutual coupling, two four element arrays were constructed.

Eight active inverted stripline antennas were built and tested for the square and diamond array. Since mutual coupling is used for injection-locking, the locking gain level between two of these active antennas would be high with a corresponding narrow locking bandwidth. Mechanical tuning of the diodes ensured that several antennas would operate within the narrow locking bandwidth. This allows the use of a single power supply at a fixed bias voltage for all diodes and successful power combining. Antennas 1, 2, 3 and 4 were used in a four element square array while antennas 5, 6, 7 and 8 were used in a four element diamond array. Table IV lists the operating frequency, oscillator power and efficiency of each antenna and array as well as the EIRP. The square array uses 17 mm spacing between elements. The diamond array spacing between elements is 17 mm along the diagonal. Fig. 6 shows the array configurations, spacing and diode position.

The power combining efficiency (η) is defined by

$$\eta = \frac{P_{combiner}}{\sum_N P_n} \times 100\% \tag{3}$$

- P_n = Power of nth active antenna (Using G_o as the gain of a single passive antenna).
- P_{combiner} = Power of injection-locked, power-combined signal (Use the gain as NG_o for an N element array).
- All oscillator power calculations use the Friis transmission equation [11].

The square array was used to test two element injection-locking and power combining via mutual coupling for E and H-plane elements. The two element H-plane array shows a power combining efficiency of 86.4% while the E-plane array's efficiency was 99.8%. The four element square array exhibited power combining efficiency of 89%. The overall DC to RF efficiency of the four element array is 1.63%. The two element patterns for E and H-plane power combining show nearly 2 to 1 beamwidth sharpening of over a single element. The antenna patterns for the square power combiner

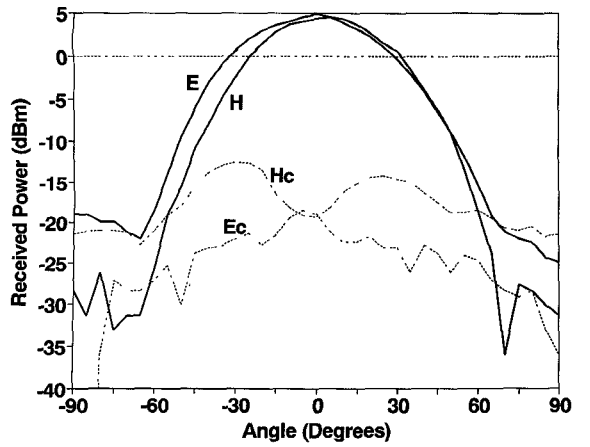

(a)

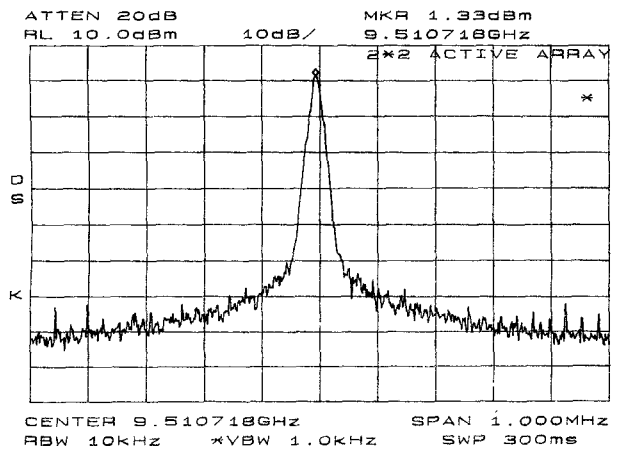

(b)

Fig. 7. The four element square array. (a) Power combiner patterns (E, H-Co-polarization; E_c, H_c-Cross-polarization. (b) Power combiner spectrum.

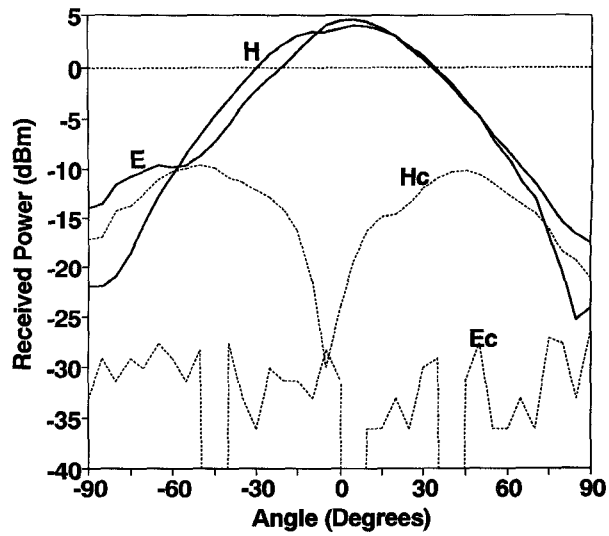

Fig. 8. The four element diamond array power combiner patterns. E, H-Co-polarization; E_c, H_c-Cross-polarization.)

array is shown in Fig. 7(a). The array can be bias tuned from 10.7 to 14 Volts without losing injection lock over a 60 MHz bandwidth from 9.467 to 9.527 GHz. The output power level varied less than 0.8 dB over the bias tuned range. The power combiner spectrum is shown in Fig. 7(b).

The four element diamond array was also tested for injection-locked power combining. The diamond array power combining efficiency is 86.57% with an overall DC to RF conversion efficiency of 1.47%. The array can be bias tuned from 9.5 to 12.2 V without losing injection lock over a 50 MHz bandwidth. The radiation patterns of the diamond array are shown in Fig. 8. The 3 dB beamwidth is similar to that of Fig. 7(a). The cross-polarization level of the square array is 3 dB lower than that of the diamond array.

VI. Beam Steering Without Conventional Phase-Shifters

Active antenna operating frequency depends on the circuit and applied bias voltage. Single-output DC power supplies are usually used to operate an entire array to reduce the overall cost. However, a variable voltage can be used to change individual active antenna operating frequencies. The difference between self-oscillating frequencies of active antennas produces a phase-shift in the injection-locked power combiner. The phase-shift can be used to electronically steer the beam of the active antenna power combiner [24].

Two identical active antennas with different bias voltages oscillate at different frequencies. When the difference between the self oscillating frequencies is within the locking-bandwidth for a given locking-gain, the antennas will injection-lock at a single oscillating frequency for power combining. A row of active antennas can be made to operate at various self-oscillating frequencies using a ramped DC voltage. The elements will injection lock and the power combiner antenna beam will steer off-broadside. The beam steering angle is directly proportional to the difference in self-oscillating frequencies which depends on the applied DC bias voltage.

The square 2 × 2 power combiner exhibited 15 degrees H-plane beam-steering. For H-plane beam steering, one bias voltage (V_1) is applied to antennas 1 and 3 (see Fig. 6), and another bias voltage (V_2) is applied to antennas 2 and 4. The self-oscillating frequencies of each antenna were adjusted to within 0.02% at 12 V bias. When $V_1 = V_2$ the resultant power combining beam is broadside at 9.511 GHz with 89% combining efficiency. The bias V_1 was then lowered to 10.5 V while maintaining V_2 at 12 V. Similarly, the bias V_2 was adjusted to 11 V while maintaining V_1 at 12 V. the two extremes give a 15 degree H-plane beam steering as shown in Fig. 9. All four elements remain injection-locked throughout the tuning range. As shown, the overall beam remains within 1.2 dB of the maximum at 0 degrees. The cross-polarization level increases slightly over the broadside combiner but remains at least 15 dB below the maximum. E-plane beam-steering can be accomplished by pairing elements 1 with 2 and 3 with 4.

VII. Conclusions

The probe-fed passive cavity enclosed inverted stripline antenna is conformal like other microstrip antennas. Furthermore, the antenna provides an inherent radome for protection and sealing. In an array environment, the enclosure provides

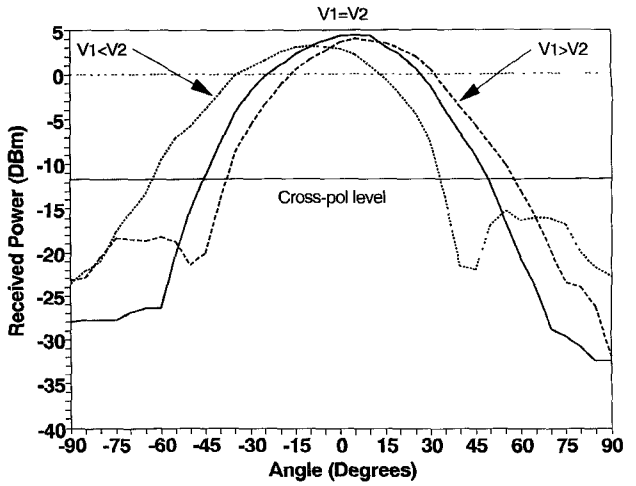

Fig. 9. Beam Steering of active antenna arrays without conventional phase-shifters.

improved isolation between elements. The overall gain is slightly higher than standard patch antennas. However, a large array of passive probe-fed elements may prove laborious without an improved corporate feeding scheme and a single probe input.

Similarly, the active antenna configuration does not require drilling through the circuit substrate or soldering to the patch antenna. The configuration allows easy optimization of frequency, power or antenna performance in a single test fixture. The operating frequency can be tuned mechanically and electronically. The antenna exhibits a purer spectrum and higher stability than current active antennas. Correct choice of the housing and dielectric insert material allows hermetic sealing of active devices below the antenna. The heat sink and enclosure provides enough metal volume for efficient dissipation of heat and improved reliability of active devices. For mm and sub-mm applications, monolithically fabricated inserts can be inserted to a machined metal housing. The design allows easy modular construction and active element replaceability.

The antenna provides a means of developing tile type arrays for reduced size and conformability. The array structure is suitable for open resonators in power combining. An array of active antennas has shown high power combining efficiencies via mutual coupling and the ability to maintain injection-locking with bias tuning for frequency modulated links or radar applications. The combiner arrays exhibit similar locking gain and bandwidth as the single element. External injection-locking provides another means of frequency tuning or modulating the operating frequency as well as improving spectral purity and frequency stability. Beam steering has also been demonstrated to further the capabilities of active antenna power combiners.

ACKNOWLEDGMENT

This investigation was funded partially by the U.S. Army Research Office and the Texas Higher Education Coordinating Board's Advanced Technology Program. The substrate material was provided by the Rogers Corporation. The authors thank Drs. Krys Michalski and Steve Wright for many helpful discussions and suggestions.

REFERENCES

[1] K. Chang and C. Sun, "Millimeter-wave power-combining techniques," *IEEE Trans. Microwave Theory Tech.*, vol. MTT-31, no. 2, pp. 91–107, Feb. 1983.

[2] J. W. Mink, "Quasi-optical power combining of solid-state millimeter-wave sources," *IEEE Trans. Microwave Theory Tech.*, vol. MTT-34, pp. 273–279, Feb. 1986.

[3] J. C. Wiltse and J. W. Mink, "Quasi-optical power combining of solid-state sources," *Microwave J.*, pp. 144–156, Feb. 1992.

[4] H. J. Thomas, D. L. Fudge and G. Morris, "Gunn source integrated with a microstrip patch," *Microwaves and RF*, pp. 87–89, Feb. 1985.

[5] T. O. Perkins, "Active microstrip circular patch antenna," *Microwave J.*, pp. 110–117, Mar. 1987.

[6] K. Chang, K. A. Hummer, and G. Gopalakrishnan, "Active radiating element using FET source integrated with microstrip patch antenna," *Electron. Lett.*, vol. 24, no. 21, pp. 1347–1348, Oct. 13, 1988.

[7] V. F. Fusco, "Series feedback integrated active microstrip antenna synthesis and characterization," *Electron. Lett.*, vol. 28, n0. 1, pp. 89–91, Jan. 2, 1992.

[8] R. A. York, R. M. Martinez, and R. C. Compton, "Hybrid transistor and patch antenna element for array applications," *Electron. Lett.*, vol. 26, pp. 494–495, Mar. 1990.

[9] P. M. Haskings, P. s. hall, and J. S. Dahele, "Active patch antenna element with diode tuning," *Electron. Lett.*, vol. 27, no. 20, pp. 1846–1847, Sept. 26, 1991.

[10] J. A. Navarro, Y. Shu, and K. Chang, "Active endfire antenna elements and power combiners using notch antennas," *IEEE MTT-S Int. Microwave Symp. Dig.*, 1990, Dallas, TX, pp. 793–796.

[11] J. A. Navarro, Y. Shu, and K. Chang, "Broadband electronically tunable planar active radiating elements and spatial power combiners using notch antennas," *IEEE Trans. Microwave Theory Tech.*, vol. MTT-40, no. 2, pp. 323–328, Feb. 1992.

[12] J. A. Navarro and K. Chang, "Broadband electronically tunable planar active radiating elements and spatial power combiners using notch antennas," (Invited Paper) *Microwave J.*, vol. 35, pp. 87–101, Oct. 1992.

[13] S. Young and K. D. Stephan, "Stabilization and power combining of planar microwave oscillators with an open resonator," *IEEE MTT-S Int. Microwave Symp. Dig.*, 1987, pp. 185–188.

[14] K. Chang, K. A. Hummer, and J. L. Klein, "Experiments on injection locking of active antenna elements for active phase arrays and spatial power combiners," *IEEE Trans. Microwave Theory Tech.*, vol. MTT-37, no. 7, pp. 1078–1084, July, 1989.

[15] J. Birkeland and T. Itoh, "Planar FET oscillators using periodic microstrip patch antennas," *IEEE Trans. Microwave Theory Tech.*, vol. MTT-37, no. 8, pp. 1232–1236, Aug. 1989.

[16] Z. B. Popovic, R. M. Weikle II, M. Kim, K. A. Potter, and D. B. Rutledge, "Bar-grid oscillators," *IEEE Trans. Microwave Theory Tech.*, vol. MTT-38, no. 3, pp. 225–230, mar. 1990.

[17] R. A. York and R. C. Compton, "Quasi-optical power combining using mutually synchronized oscillator arrays," *IEEE Trans. Microwave Theory Tech.*, vol. MTT-39, no. 6, pp. 1000–1009, June 1991.

[18] ——, "Dual-device active patch antenna with improved radiation characteristics," *Electron. Lett.*, vol. 28, no. 11, pp. 1019–1021, May 1992.

[19] F. Abboud, J. P. Damiano, and A. Papiernik, "A new model for calculating the input impedance of coax-fed circular microstrip antennas with and without air gaps," *IEEE Trans. Antennas Propagat.*, vol. 38, no. 11, pp. 1882–1885, Nov. 1990.

[20] P. Pramanick and P. Bhartia, "CAD models for millimeter-wave finlines and suspended-substrate microstrip lines,"*IEEE Trans. Microwave Theory Tech.*, vol. MTT-33, no. 12, pp. 1429–1435, Dec. 1985.

[21] J. A. Navarro, K. Chang, J. Tolleson, S. Sanzgiri, and R. Q. Lee, "A 29.3 GHz cavity enclosed aperture-coupled circular patch antenna for microwave circuit integration," *IEEE Microwave Guided Wave Lett.*, vol. 1, no. 7, pp. 170–171, July 1991.

[22] S. Sanzgiri and J. Tolleson, "*Ka* band sub-array technology demonstration program," *Texas Instruments Design Review*, Aug. 7, 1991.

[23] R. Alder, "A study of locking phenomena in oscillators," *Proc. IRE*, vol. 34, pp. 351–357, June 1946.

[24] J. A. Navarro and K. Chang, "Beam steering of active antenna arrays," *Electron. Lett.*, vol. 29, no. 3, pp. 302–304, February 4, 1993.

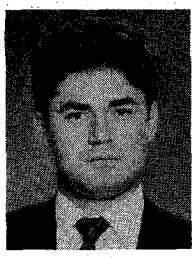

Julio A. Navarro was born in Cordoba, Argentina on November 13, 1964. He received the B.S. and M.S. degrees in electrical engineering from Texas A&M University in 1988 and 1990, respectively.

He has been a co-operative education student with General Dynamics-Fort Worth from May, 1985 to February, 1991. At General Dynamics, he worked for Avionics Systems Design, Advanced Technology & Systems Engineering, Field Engineering: Emitters & Intelligence, Antenna Systems and Radar Cross-Section Research groups. At Texas A&M University, he has been a research and teaching assistant since January 1991. His teaching assistant duties included 'Ultra-High Frequency Techniques' course lab as well as many senior student projects. As a research assistant, he has introduced active endfire notch radiators, Gunn VCOs and PIN switchable & varactor-tunable uniplanar filters. He has also introduced tunable slotline and CPW ring resonators. He has developed Ka-band aperture-coupled circular patch antennas for a NASA-Lewis/Texas Instruments-Mckinney project. He is currently working on active antenna elements for Quasi-optical power combining in phased-arrays. He is a Ph.D. candidate under the direction of Professor Kai Chang.

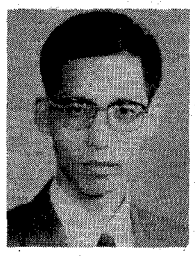

Lu Fan received the B.S. degree in electrical engineering from Nanjing Institute of Technology (current name Southeast University), Nanjing, China, in 1982. From September 1982 to December 1990, he was with the Department of Radio Engineering of Nanjing Institute of Technology as a teaching assistant and lecturer.

In January 1991, he became a Research Associate in the Department of Electrical Engineering, Texas A&M University, College Station, TX. His research interests include microwave and millimeter-wave components and circuits.

Kai Chang (S'75–M'76–SM'85–F'91) for photograph and biography, see this issue, p. 1709.